Electric monopole transitions and structure of low-spin states in ^{106}Pd

N. Marchini,[1,2] A. Nannini,[2] M. Ottanelli,[2] A. Saltarelli,[1,3] G. Benzoni,[4] E. R. Gamba,[5,*] A. Goasduff,[6] A. Gottardo,[6] J. Ha,[7] T. Krings,[8] M. Perri,[1,3] M. Polettini,[4,9] M. Rocchini,[10] and P. Sona[2]

[1]*Università degli Studi di Camerino, Dipartimento di Fisica, IT-62032 Camerino, Italy*
[2]*INFN Sezione di Firenze, IT-50019 Firenze, Italy*
[3]*INFN Sezione di Perugia, IT-06123 Perugia, Italy*
[4]*INFN Sezione di Milano, IT-20133 Milano, Italy*
[5]*Museo Storico della Fisica e Centro Studi e Ricerche Enrico Fermi, IT-00184 Roma, Italy*
[6]*INFN Laboratori Nazionali di Legnaro, IT-35020 Padova, Italy*
[7]*Dipartimento di Fisica, Università degli Studi di Padova and INFN, IT-35122 Padova, Italy*
[8]*Institut für Kernphysik (IKP), D-52428 Jülich, Germany*
[9]*Università degli Studi di Milano, Dipartimento di Fisica, IT-20133 Milano, Italy*
[10]*University of Guelph, Department of Physics, N1G2W1 Guelph, Canada*

(Received 3 February 2022; accepted 15 April 2022; published 9 May 2022)

Structures in the ^{106}Pd nucleus have been studied in the EC/β^+ decay of ^{106}Ag at the INFN Legnaro National Laboratories using the Spes Low-energy Internal Conversion Electron Spectrometer (SLICES). The K-conversion coefficients and the electric monopole transition strengths, between low-lying 2^+ and 0^+ states, have been studied. These experimental data combined with the results from conversion electron measurement on ^{104}Pd previously performed by the Florence spectroscopy group were compared with the theoretical values calculated in the framework of the interacting proton-neutron boson model. Good agreement between experimental and theoretical values is found when interpreting the 0^+_3 level as an intruder state.

DOI: 10.1103/PhysRevC.105.054304

I. INTRODUCTION

The collective properties of stable Pd isotopes (Z=46) have been the focus of several experimental and theoretical studies in the past decades [1–4]. They have been considered as "transitional" nuclei, displaying a character that varies from vibrational to γ unstable. Indeed, detailed analyses (see Refs. [5,6]) provided a good description of even-mass Pd nuclei as pertaining to a region of transition from the vibrational U(5) limit to the γ-soft O(6) limit of the IBA-2 model [7].

This interpretation was recently questioned in a systematic study of the even mass isotopes of Mo, Ru, Pd, Cd, and Te [8]. The authors concluded that the existence of low-energy quadrupole vibrations in some of these nuclei must be questioned and that the study of collective states must involve not only electromagnetic observables such as B(E2) values and quadrupole moments, which by definition only sample the charge and/or current distributions, but also other electromagnetic probes that are sensitive to shape coexistence and configuration mixing, such as, for instance, the electric monopole (E0) transitions.

The question of whether Pd nuclei may actually exhibit a nearly harmonic quadrupole structure was recently addressed by two experiments involving the neutron inelastic scattering, devoted to the study of the structure of the ^{106}Pd isotope [9,10]. In the first one, a characterization of the low-lying excited states up to ≈2.4 MeV for spin ⩽6 was obtained. The level scheme was organized into rotational bands, each characterized by a definite value of K. In the second experiment, on the basis of previously measured internal conversion electron [11] and new lifetime data, the strength of E0 transitions between 2^+ states was determined. The authors concluded that the extracted monopole transition strength values provide evidence for shape coexistence between the bands with the same K value.

The existing data on converted transitions in the ^{106}Pd isotope are somewhat limited and affected by a large uncertainty: For instance, two values differing by a factor ≈3 are available for the internal conversion coefficient of the $2^+_3 \longrightarrow 2^+_1$ transition, thus preventing a definite conclusion on the amount of mixing between these two levels.

The aim of the present work is to provide further information to better understand the structure of low-lying states in the Pd isotopes with N0. The E0 transitions between both 0^+ and 2^+ states in ^{106}Pd have been studied in electron spectroscopy experiment employing our recently developed apparatus [12]. The new data, combined with those obtained in the re-analysis of data previously acquired on ^{104}Pd by the nuclear spectroscopy group in Florence, help to clarify the properties of the 0^+ and 2^+ states up to 2.3 MeV in the ^{104,106}Pd isotopes.

II. EXPERIMENTAL DETAILS

A dedicated experiment to study the structure of ^{106}Pd at low excitation energy was performed at the INFN

*Current address: Dipartimento di Fisica, Università degli Studi di Milano and INFN, 20133 Milano, Italy

TABLE I. Experimental K-internal conversion coefficients α_K for transitions in ^{106}Pd compared with the calculated values [14].

		$\alpha_K \times 10^3$		
$J_i^\pi \longrightarrow J_f^\pi$	E_γ (keV)	Experiment	Theory (E2)	Theory (M1)
$2_2^+ \longrightarrow 2_1^+$	616	2.97(11)	2.89	2.97
$2_2^+ \longrightarrow 0_1^+$	1128	0.64(9)	0.68	
$2_3^+ \longrightarrow 2_1^+$	1050	1.06(7)	0.79	0.89
$0_2^+ \longrightarrow 2_1^+$	621	2.6(2)	2.8	
$0_3^+ \longrightarrow 2_1^+$	1195	0.71(13)	0.60	
$0_4^+ \longrightarrow 2_2^+$	873	1.23(8)	1.20	

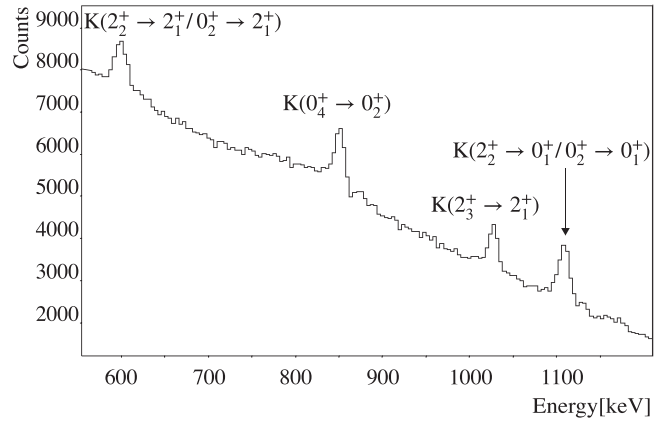

FIG. 1. Section of the ^{106}Pd SLICES energy spectrum; K-conversion lines are labeled with spin and parity of the initial and final levels.

Legnaro National Laboratories (LNL) in Italy. The excited states in the nucleus of interest were fed in the EC-β^+ decay of ^{106g}Ag ($T_{1/2} = 24$ min) and ^{106m}Ag ($T_{1/2} = 8$ d) produced via the (p, n) reaction on a self-supporting 3-mg/cm^2-thick ^{106}Pd target enriched to 96%. The 5.5-MeV proton beam was delivered by the LNL Van der Graaff CN accelerator [13] with an average intensity of 200 nA. To favor the fast decay activity of ^{106}Ag, which populates the 0^+ levels in ^{106}Pd, measurements have been performed by alternating bombarding and measuring periods of 35 min. A 5-min waiting time was inserted to allow the decay of the short-lived ^{108}Ag ($T_{1/2} =$ 3.4 min) produced in the (p, n) reaction on the 1% ^{108}Pd isotope present in the target. The ^{108}Ag beta decays mostly (95%) to the ground state of ^{108}Cd [$Q(\beta^-) = 1650(7)$ keV] increasing the background in the electron spectra. By inserting the above-mentioned waiting time this background is reduced by a factor ≈4 while only 10% of the ^{106}Ag activity is lost. The only other contaminant present in the target that can significantly contribute to the background is the ^{105}Pd isotope (2%). However, no transitions related to the ^{105g}Ag EC decay are visible in the spectrum.

The internal conversion electrons emitted in the deexcitation of the states populated in the decay of ^{106g}Ag were detected by the SLICES spectrometer [12], used for the first time in the present experiment. SLICES setup utilizes a 6.8-mm-thick segmented lithium-drifted silicon detector coupled to a magnetic transport system to guide the electrons around a central photon shield towards the detector. The efficiency of the spectrometer can be optimized by changing the shape of the magnetic transport system components. For the configuration adopted in this experiment, the maximum detection efficiency of 12% is obtained at 1 MeV. The adopted configuration and the related efficiency curve have been studied in detail in Ref. [12]. An HPGe detector with an energy resolution of 2.4 keV (FWHM) at 1.3 MeV was used to detect γ rays deexciting the nuclear states.

III. RESULTS

Conversion electron measurements have been performed to determine K-conversion coefficients α_K and to evaluate the monopole strength ρ^2 of E0 transitions between states having the same spin and parity. The α_K values obtained for the transitions of interest are summarized in Table I. The agreement between the experimental and the theoretical values for pure E2 transitions on one hand is a test of the reliability of SLICES apparatus in performing in-beam measurements, and on the other hand, of the correct determination of $\alpha_K(2_3^+ \longrightarrow 2_1^+)$. Two different α_K values for this transition are reported in the literature [11,15]. The value obtained in the present work is in agreement with the one determined in Ref. [11].

TABLE II. A comparison between the E0 transition strengths ρ^2 and q^2(E0/E2) extracted in the present work together with literature values for ^{106}Pd. Transition energy, lifetimes for the initial states, multipole mixing ratios δ(E2/M1), and branching ratios B R are taken from Ref. [9] and references therein.

					q^2(E0/E2)		$\rho^2 \times 10^3$	
$J_i^\pi \longrightarrow J_f^\pi$	E_γ (keV)	τ (fs)	$\delta(E2/M1)$	B R	Present	Previous	Present	Previous
$0_2^+ \longrightarrow 0_1^+$	1134	8400(1900)			0.166(15)	0.162(7)[a]	17(4)	16.4(40)[b]
$0_3^+ \longrightarrow 0_1^+$	1706	4000(700)			0.09(15)		2(4)	<3[b]
$0_4^+ \longrightarrow 0_1^+$	2001	>1200			0.124(18)		<19	
$0_4^+ \longrightarrow 0_2^+$	867	>1200			0.22(6)		<90	
$2_2^+ \longrightarrow 2_1^+$	616	4500(360)	-8.7^{+17}_{-19}	0.647(24)	0.027(38)		5(8)	
$2_3^+ \longrightarrow 2_1^+$	1050	1900(190)	0.24(1)	0.853(34)	4.2(18)	5.8(33)[a]	26(11)	34(22)[b]

[a]Reference [16].
[b]Reference [10].

The experimental $\alpha_K(2_3^+ \longrightarrow 2_1^+)$ value, large with respect to the calculated one, suggests the presence of a strong E0 component in this transition. The section of the electron spectrum in the energy range around 1 MeV is shown in Fig. 1. The K-conversion electron peak of the $2_3^+ \longrightarrow 2_1^+$ transition is in a clean region of the spectrum.

Conversion-electron measurements can also provide information on the ρ^2. For a transition between states with $J_i^+ = J_f^+ = 0$, it is related to the ratio,

$$q^2_{ifj} = I_K(E0; 0_i^+ \rightarrow 0_f^+)/I_K(E2; 0_i^+ \rightarrow 2_j^+), \quad (1)$$

between the intensity of the E0 and E2 K-conversion lines deexciting a given 0_i^+ level. The E0 strength can be determined via the expression,

$$\rho^2(J_i^+ \rightarrow J_f^+) = q^2_{ijf}(E0/E2) \times \frac{\alpha_K(E2)}{\Omega_K(E0)} \times W_\gamma(E2), \quad (2)$$

where Ω_K(E0) is the electronic factor for the K conversion of the E0 transition obtained from Ref. [14], α_K(E2) is the K-conversion coefficient for the E2 transition, and W_γ(E2) is the γ-ray E2 transition probability.

In the case of $J_i^+ = J_f^+ \neq 0$, the E0 and E2 transitions in Eq. (1) connect the same initial and final levels. Because the contributions owing to the different multipolarities to the same transition are indistinguishable, $q^2_{ijf}(E0/E2)$ is extracted from the internal conversion coefficient, which in the case of mixed E0, E2, and M1 multipolarities, has the expression:

$$\alpha_K = \frac{\alpha_K^{\text{th}}(M1) + (1 + q^2_{ifj})\delta^2\alpha_K^{\text{th}}(E2)}{(1 + \delta^2)}, \quad (3)$$

where δ is the (E2/M1) mixing ratio, and $\alpha_K^{\text{th}}(M1)$, $\alpha_K^{\text{th}}(E2)$ are the theoretical values of the internal conversion coefficient from the Band-Raman Internal Conversion Coefficents (BRICC) database [14].

The q^2(E0/E2) and ρ^2 values extracted in the present work are summarized in Table II. The analysis of the $2_2^+ \longrightarrow 2_1^+$ K-electron line at 622 keV was made difficult by the presence of the predominant 616-keV peak because of the K-conversion electrons of the $0_2^+ \longrightarrow 2_1^+$ transition. As a consequence, the obtained $q^2(2_2^+ \longrightarrow 2_1^+)$ value has a large uncertainty. The coupling of SLICES with an HPGe detector allows us not only to extract the internal conversion coefficients but also to study in detail the decay scheme of the levels in ^{106}Pd. An example of the γ-ray energy spectrum is shown in Fig. 2, where the transitions relevant to this work are shown. The part of the spectrum below 300 keV is dominated by the Compton edge of the 511-keV annihilation transition, which also covers the 512-keV, $2_1^+ \longrightarrow 0_1^+$ transition in ^{106}Pd. Figure 3 shows the partial level scheme of ^{106}Pd up to an energy of ≈2.3 MeV with branching ratios obtained in the present work. The ^{106}Pd nucleus was recently studied via a $(n, n'\gamma)$ reaction [9], where a number of new transitions were reported. In the present work, the existence of the $2_4^+ \longrightarrow 2_3^+$, $2_4^+ \longrightarrow 3_1^+$, and $2_4^+ \longrightarrow 2_2^+$ transitions at 347 keV, 352 keV, and 782 keV, respectively, cannot be confirmed as they are below the observational limit. The area of the peak at 680 keV is higher than expected on the basis of the intensities reported in [17] for

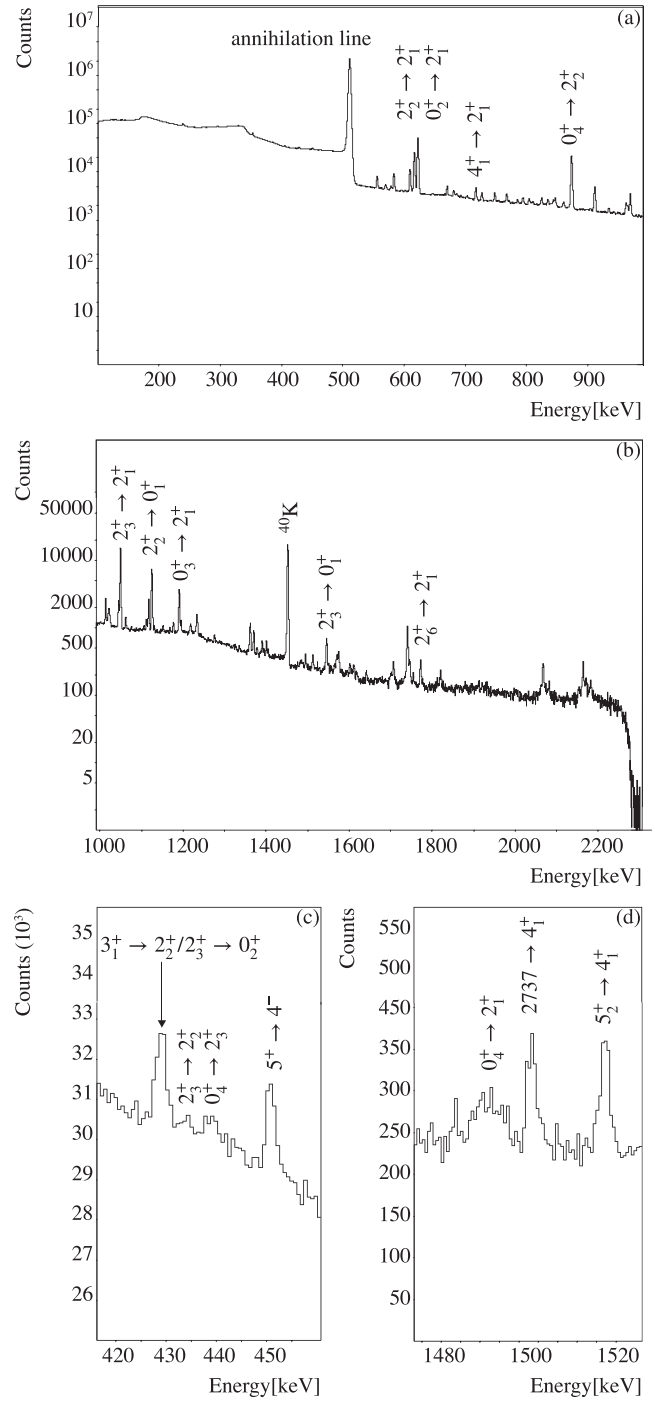

FIG. 2. Sections of the ^{106}Pd γ-ray energy spectrum. (a) The 100- to 1000-keV energy range. (b) The 1000- to 2300-keV energy range. Both panels have the vertical axes in the logarithmic scale. The lower panels (c) and (d) show the regions around 450 keV and 1500 keV respectively. Most intense peaks of interest are labeled with spin and parity of the initial and final levels.

the well-known $2_5^+ \longrightarrow 2_3^+$ and $5_2^+ \longrightarrow 4_3^+$ transitions. A possible contribution could arise from the proposed $2_4^+ \longrightarrow 4_1^+$ transition at 681 keV as proposed in [9]. A 439-keV transition from the 0_4^+ state to the 2_3^+ state is visible in the γ-ray energy spectrum [see Fig. 2(c)]. A small peak at 1490 keV was

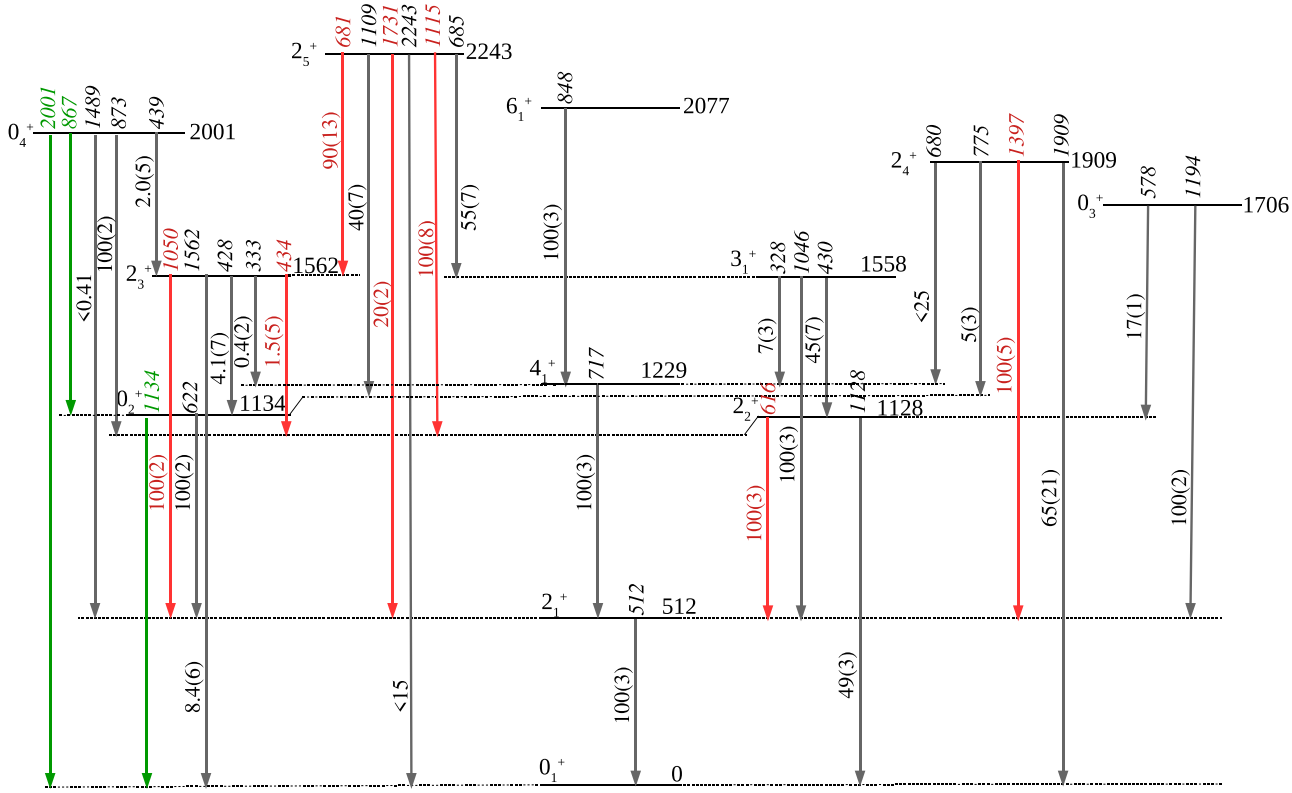

FIG. 3. Low-lying level scheme in ^{106}Pd. The observed γ transitions with the related branching ratios extracted in this experiment are reported on the arrow. The observed E0 transitions between the excited 0^+ states are reported in green. The transition with mixed E0, E2, and M1 multipolarities are presented in red.

assigned to the $0_4^+ \longrightarrow 2_1^+$ transition [see Fig. 2(d)]. Both these transitions were previously reported in Refs. [17,18].

The Florence spectroscopy group had performed measurements of internal conversion electrons to investigate E0 transitions in ^{104}Pd [19]. The deduced E0 strengths are reported in Table III. In the same experiment, $\gamma - \gamma$ coincidences have been also measured. We have now reanalyzed the data to gain a deeper insight on the existence of a 0_4^+ state, reported in Refs. [17,18] at 2103(2) keV. This level was seen only in a (p, p') reaction and no information is given on its decay properties. In the γ-ray spectrum acquired in coincidence with the 786-keV $2_2^+ \longrightarrow 2_1^+$ transition, a small peak is visible (see. Fig. 4) at 759.3(5) keV. Assuming that the peak corresponds to the $0_4^+ \longrightarrow 2_2^+$ transition, the energy of the initial level would be 2101 keV. We looked for transitions from the potential 0_4^+ state at 2101 keV to the 2_1^+ state and to the 0_2^+ and 0_3^+ states. The energies of the corresponding transitions would be 1545 keV, 743 keV, and 283 keV, respectively. A new 1545.2(3)-keV transition was indeed identified in Ref. [19] but was assigned to the decay from the 2868.7-keV level. The 743-keV E0 transition in our data would be completely covered by the much more intense K-conversion line of the 768-keV, $4_1^+ \longrightarrow 2_1^+$ transition, while a small peak at 284 keV is visible in the electron spectrum of Fig. 5. Because in the corresponding γ-ray energy spectrum (Fig. 5, lower panel), there is no peak at an energy $\approx$308 keV (while the peak corresponding to the 289-keV transition from the 4^+ level at 3158 keV is clearly visible) we tentatively

TABLE III. Experimental values of ρ^2 in ^{104,106}Pd and in ^{100,102}Ru compared to theoretical ones evaluated using the Hamiltonian parameters from Ref. [6] and the E0 effective charges $\beta_{0\nu} = 0.194\ e\ fm^2$, $\beta_{0\pi} = 0.009\ e\ fm^2$ deduced in the present work. The values marked by an asterisk have been used in the χ^2 minimization procedure.

Nuclide	$J_i^\pi \longrightarrow J_f^\pi$	E_γ (keV)	$\rho^2_{\rm exp} \times 10^3$		$\rho^2_{\rm calc} \times 10^3$
^{104}Pd	$0_2^+ \longrightarrow 0_1^+$	1334	11(2)[a]	*	10
^{104}Pd	$2_2^+ \longrightarrow 2_1^+$	786	5(4)[b]	*	1
^{106}Pd	$0_2^+ \longrightarrow 0_1^+$	1134	17(4)[c]	*	16
^{106}Pd	$0_4^+ \longrightarrow 0_1^+$	2001	<19[c]		0.3
^{106}Pd	$0_4^+ \longrightarrow 0_2^+$	867	<90[c]		4
^{106}Pd	$2_2^+ \longrightarrow 2_1^+$	616	5(8)[c]		1
^{106}Pd	$2_3^+ \longrightarrow 2_1^+$	1050	26(11)[c]	*	28
^{106}Pd	$2_4^+ \longrightarrow 2_1^+$	1398	21^{+10}_{-21}[d]		0.1
			18^{+10}_{-18}[d]		
^{106}Pd	$2_5^+ \longrightarrow 2_2^+$	1115	96^{+43}_{-61}[d]		18
^{100}Ru	$0_2^+ \longrightarrow 0_1^+$	1130	10.3(18)[e]	*	11.4
^{102}Ru	$0_2^+ \longrightarrow 0_1^+$	944	14(3)[e]	*	17

[a]Reference [19].
[b]Calculated in the present work from the data of Ref. [19].
[c]Present work.
[d]Reference [16].
[e]Reference [26]

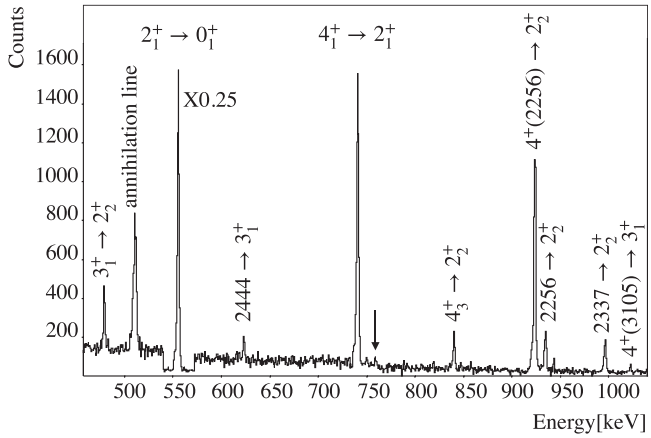

FIG. 4. Section of the ^{104}Pd γ-ray energy spectrum gated on the 786-keV, $2_2^+ \longrightarrow 2_1^+$ transition showing the region around 750 keV. A small peak is visible at an energy of 759 keV (indicated by the arrow). The $2_1^+ \longrightarrow 0_1^+$ transition at 556 keV was normalized.

assign the transition with E0 multipolarity. Consequently, the spin and parity of the 2101-keV state in ^{104}Pd is restricted to $J^\pi = 0^+$.

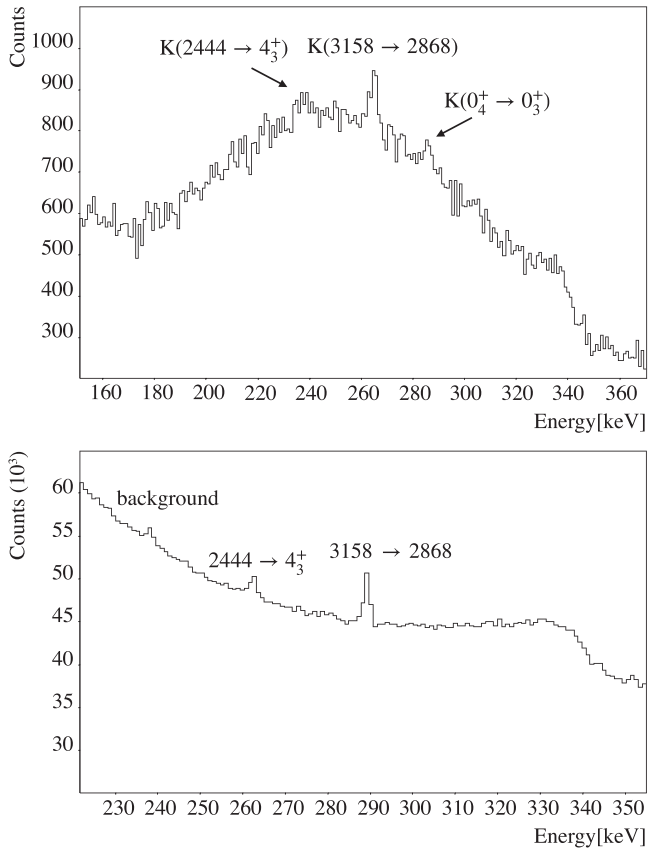

FIG. 5. Sections of the ^{104}Pd electron and γ-ray energy spectra. (Upper panel) Section of the electron energy spectrum in the 160- to 360-keV energy range. The small peak visible at an energy of 284 keV was assigned to the $0_4^+ \longrightarrow 0_3^+$ transition. (Lower panel) Portion of the γ-ray energy spectrum in the 230- to 350-keV energy range. No peak is visible above the line corresponding to the 289 keV transition from the 4^+ level at 3158 keV.

IV. DISCUSSION

The interpretation of the low-lying levels in even-mass Pd isotopes is still controversial and different models have been employed to describe their intrinsic configurations. In the present work, we consider the contribution that the study of E0 transition can provide to clarify the structure of the low-lying states in $^{104-106}$Pd.

The excitation energy pattern of the low-lying states in the $^{104-106}$Pd isotopes might suggest a vibrational structure, with a triplet of states with $J^\pi = 0^+, 2^+, 4^+$ whose energy is approximately twice that of the first excited 2^+ state. However, the B(E2) values of transitions from these states to the 2_1^+ cast some doubts on their vibrational character. The values of the $B(E2; I^\pi \to 2_1^+)$ for the decays of the two-phonon states ($0^+, 2^+, 4^+$) should be identical and twice the value of the $B(E2; 2_1^+ \to 0_1^+)$ one-phonon decay; instead they differ considerably and are smaller than expected (see Fig. 6).

As to the identification of the three-phonon quintuplet, it is made difficult by the presence of additional levels with $J^\pi = 0^+, 2^+$. They have been considered as intruder states resulting from proton-pair excitations across the $Z = 50$ shell. Two signatures are commonly given for the identification of intruder states: (i) the characteristic V-shape pattern of their excitation energies versus neutron number, and (ii) the enhanced cross-section for single- and two-nucleon transfer reactions with respect to those between collective states. Low-lying intruder configurations have been studied in even-even Pd isotopes in Refs. [20,21]. Here it is suggested that the experimental 0_3^+ and 2_4^+ states have intruder character until N=60 and again for N=70, while the 0_2^+ and 2_3^+ states have to be considered intruder for N=62,64. Within this hypothesis, the V-shaped pattern of the excitation energy is granted. The interpretation of the 0_3^+ states as intruder states in ^{104,106}Pd isotopes was also supported in Ref. [6] by the analysis of their decay properties. The only available data for the (^{3}He, n) transfer reaction is an upper limit for the cross-section to the 0_2^+ for N=58 isotope reported in Ref. [22], which is much smaller than the ground-state to ground-state cross-section in ^{104}Pd and ^{106}Pd.

A detailed analysis of excitation energy patterns and electromagnetic properties of positive-parity levels in even $^{100-116}$Pd ($Z = 46$) was performed some years ago [6] in the framework of the IBA-2 model, which is particularly suitable to study the evolution of an isotopic chain as a function of the neutron number. In that work, all the excitation energies and electromagnetic properties, available at the time for the low-lying levels in the even $^{100-116}$Pd isotopes, were investigated, with the exception of E0 transitions. An analogous study had been also performed by the same authors in the even $^{98-114}$Ru isotopes [23]. The IBA-2 parameters were requested to vary smoothly along each isotopic chain and among isotones in neighboring isotopic chains. An overall satisfactory agreement was obtained. The conclusion was that the even palladium isotopes could be considered as lying close to a transitional region between the vibrational U(5) limit to the γ-soft O(6) limit of the IBA-2 model.

More recently a new IBA-2 work was published [24], which uses the parameters of Ref. [6] to study the large

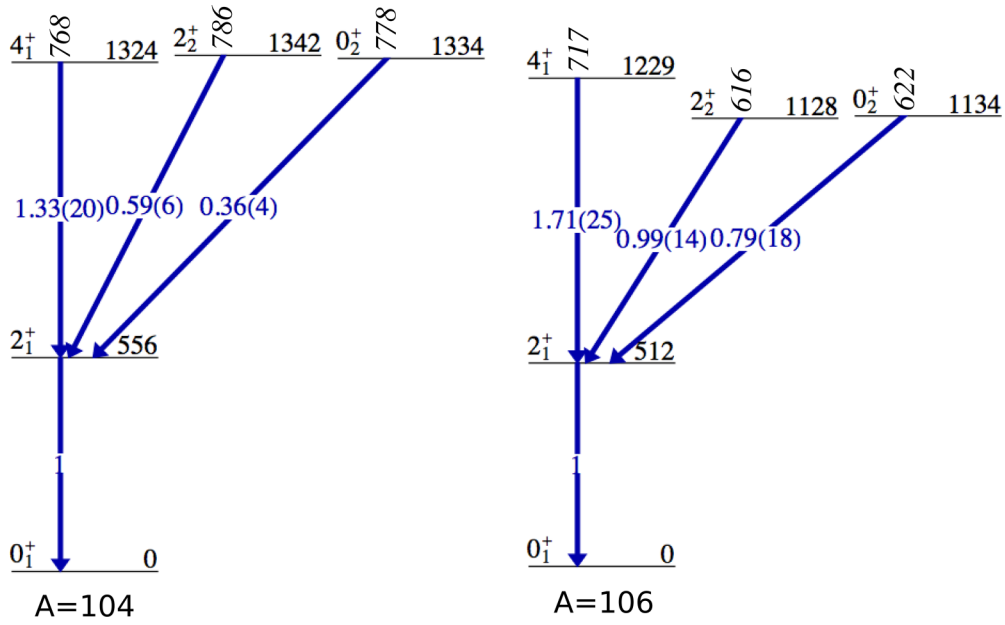

FIG. 6. Low-lying levels in even-mass ^{104,106}Pd isotopes. The B(E2) transition strengths normalized to the B(E2; $2_1^+ \rightarrow 0_1^+$) value are reported on the arrows. Data are taken from Refs. [17,18].

body of new experimental data that has become available over the years on the even Pd isotopes. In this analysis, which is mainly centered on the γ-vibrational band structure, also all the known quadrupole moments were taken into account. A comparison between the available experimental values (from Refs. [17,18]) and the calculated values from Ref. [24] of the Q normalized to the $Q(2_1^+)$ for the 2_2^+ and 4_1^+ levels is reported in Fig. 7. The agreement is good and the calculations are able to correctly predict the inversion of sign measured for the $Q(2_2^+)$. An interpretation very different from that of Refs. [6,24] was given in Ref. [8]. Here, the authors compare the properties of the low-lying states of $^{102-110}$Pd with the predictions of the harmonic vibrator and it is underlined that in none of the considered Pd isotopes the B(E2) values

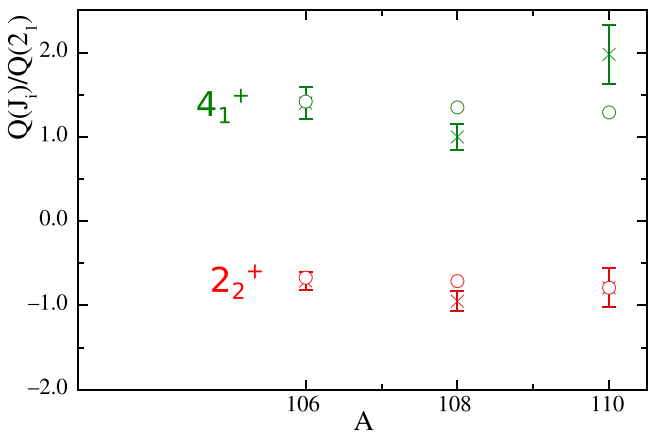

FIG. 7. Normalized experimental (crosses) and calculated (open circles) quadrupole moments of $Q(J_i)$ for the 2_2, 4_1 states as a function of mass number plotted in green and red, respectively. The values are taken from Ref. [24].

of the transitions feeding the 2_1^+ state meet the vibrational requirements. The conclusion is that the harmonic spherical vibrator interpretation breaks down already at the two-phonon levels. In particular, in the ^{106}Pd isotope the author assigns the 0_2^+ state as the head of an intruder shape-coexisting band (in agreement with Ref. [9]) while the 2_5^+ is suggested to be the member of a γ band built on the 0_2^+ state.

To further clarify to what extent the interpretation of the Pd isotopes in the framework of the IBA-2 model is valid, we performed an analysis of the available experimental data on the E0 transition between the low-lying states in $^{104-106}$Pd. The analysis was performed by using the Hamiltonian and the parameters of Ref. [6]. The Hamiltonian was diagonalized in the $U_{\pi,\nu}(5)$ basis, using the NPBOS code [25], which gives in its output the d-boson number components for each state. Excitation energies, E2 and M1 transitions in ^{104,106}Pd isotopes have been already investigated in detail in Ref. [6]. In the present work, we limited the analysis to the monopole strengths between low-lying 0^+ and 2^+ levels, which were not previously considered.

In the IBA-2 model the E0 transition operator has the expression [7],

$$\begin{aligned}\hat{T}(E0) &= \beta_{0\nu}\hat{T}_\nu(E0) + \beta_{0\pi}\hat{T}_\pi(E0) \\ &= \beta_{0\nu}(d_\nu^\dagger \times \tilde{d}_\nu)^{(0)} + \beta_{0\pi}(d_\pi^\dagger \times \tilde{d}_\pi)^{(0)}, \end{aligned} \tag{4}$$

$$\begin{aligned}\rho^2(J_i^+ \rightarrow J_f^+) = \frac{Z^2}{e^2R^4}[&\beta_{0\nu}\langle J_f|\hat{T}_\nu(E0)|J_i\rangle \\ &+ \beta_{0\pi}\langle J_f|\hat{T}_\pi(E0)|J_i\rangle]^2, \end{aligned} \tag{5}$$

where $R = 1.2\ A^{1/3}$ fm, and the parameters $\beta_{0\nu}$ and $\beta_{0\pi}$ are expressed in e fm^2.

One of the biggest difficulties in the study of the E0 transitions is related to the lack of systematics on the values of the E0 effective charges, which prevents defining a range of

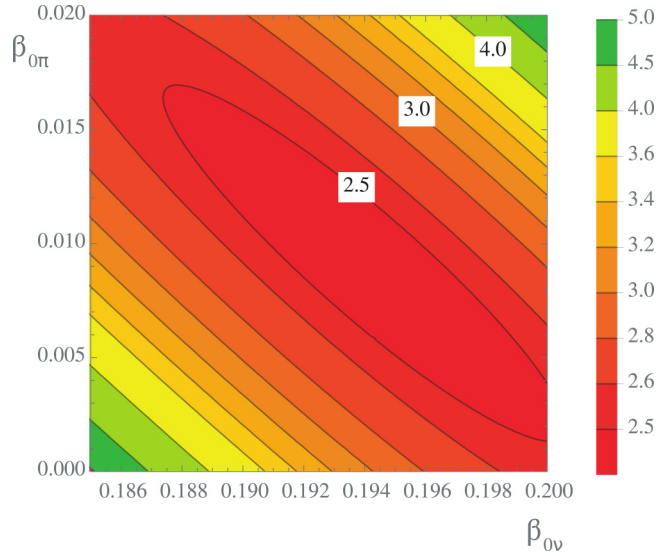

FIG. 8. Contour plot for the reduced χ^2 variable based on the comparison of theoretical and experimental ρ^2 values as a function of the effective monopole charges $\beta_{0\nu}$ and $\beta_{0\pi}$ (in e fm^2).

proper values. In the present work, in order to evaluate the effective monopole charges, the experimental data on ρ^2 have been compared with the corresponding theoretical values by performing a standard χ^2 minimization procedure restricted to the range $[-1,+1]$ e fm^2. The ρ^2 values used in the comparison are marked with asterisks in Table III. We included the $\rho^2(0_2^+ \longrightarrow 0_1^+)$ values measured in the isotone ^{100,102}Ru nuclei to further constrain the minimization procedure.

In the comparison we assumed that the intruder 0^+ state is the 0_3^+ state in ^{104,106}Pd. In Fig. 8 the contour plot for the normalized χ^2 is shown. The minimum is centered at $\beta_{0\nu} = 0.194$ e fm^2 and $\beta_{0\pi} = 0.009$ e fm^2.

By using these values for the effective monopole charges we have calculated the ρ^2 reported in Table III. Limiting our considerations to the Pd isotopes, we note the agreement between experimental and calculated values of the ρ^2 for the transition de-exciting the 0_2^+ states, supporting the interpretation of this state as the 0^+ state with $n_d = 2$ predicted by the IBA-2 model. Also for the 2_2^+ state, we observe that the IBA-2 calculations of the ρ^2 values do not contradict the interpretation of these states as the 0^+, 2^+ of the $n_d = 2$ triplet. Concerning the observed 0_4^+ state in ^{106}Pd, the calculated $\rho^2(0_4^+ \longrightarrow 0_1^+)$ value is much smaller than the $\rho^2(0_4^+ \longrightarrow 0_2^+)$ one as suggested by the experimental limits. A comparison of the experimental and calculated B(E2) values for transitions de-exciting the 0_4^+ state is made in Table IV. The experimental values for the transitions de-exciting the 0_4^+ state are calculated using the limit on the lifetime recently reported in Ref. [9] and the branching ratios obtained in the present work. The 0_4^+ state preferentially de-excites to the 2_2^+ state as expected for the member of the $n_d = 3$ quintuplet. In the present work hints for the existence of the fourth experimental 0^+ state at 2101 keV in ^{104}Pd is presented. No experimental B(E2) values from this level are known.

The agreement found between the calculated and experimental $\rho^2(2_3^+ \longrightarrow 2_1^+)$ values seems to exclude the interpretation of this state as a member of an intruder band. Because also all the other electromagnetic properties of this state were reasonably reproduced by the calculations in

TABLE IV. The experimental B(E2) and B(M1) values for the transitions de-exiciting the 0_4^+, 2_4^+, and 2_5^+ levels in ^{106}Pd. The experimental data are taken from Ref. [9] apart from the values for the 0_4^+ state (see text for more details). The theoretical values have been evaluated using the parameters from Ref. [6].

$J_i^\pi \longrightarrow J_f^\pi$	E_γ (keV)	$B(E2)_{\rm exp}$ (10^{-4} e^2b^2)	$B(E2)_{\rm calc}$ (10^{-4} e^2b^2)	$B(M1)_{\rm exp}$ (10^{-3} μ_N^2)	$B(M1)_{\rm calc}$ (10^{-3} μ_N^2)
$0_4^+ \longrightarrow 2_3^+$	439	<32	30		
$0_4^+ \longrightarrow 2_2^+$	873	<1600	1500		
$0_4^+ \longrightarrow 2_1^+$	1489	<2	3		
$2_4^+ \longrightarrow 2_3^+$	347	3600^{+2400}_{-3600}	14		
$2_4^+ \longrightarrow 4_1^+$	680	155^{+9}_{-8}	240		
$2_4^+ \longrightarrow 0_2^+$	776	60^{+36}_{-30}	515		
$2_4^+ \longrightarrow 2_2^+$	782	13^{+12}_{-8}	230	$0.13^{+0.29}_{-0.10}$	7×10^{-4}
$2_4^+ \longrightarrow 2_1^+$	1397	$0.4^{+0.4}_{-0.2}$	2	$7.3^{+4.2}_{-3.8}$	5.1
		36^{+23}_{-20}	2	$2.8^{+2.2}_{-1.6}$	5.1
$2_4^+ \longrightarrow 0_1^+$	1909	$5.7^{+3.3}_{-3.0}$	0.4		
$2_5^+ \longrightarrow 2_3^+$	680	1400^{+900}_{-700}	680	42^{+43}_{-32}	0.543
$2_5^+ \longrightarrow 3_1^+$	684	1600^{+690}_{-600}	44	$3.8^{+3.8}_{-2.0}$	0.10
$2_5^+ \longrightarrow 0_2^+$	1109	160^{+6}_{-7}	1		
$2_5^+ \longrightarrow 2_2^+$	115	100^{+150}_{-70}	1.7	19^{+15}_{-11}	0.87
$2_5^+ \longrightarrow 2_1^+$	1731	5.0^{+25}_{-21}	1.2	0.177^{+22}_{-11}	0.7
		$(6^{+155}_{-6}) \times 10^{-3}$	1.2	$(1.20^{+47}_{-42}) \times 10^{-3}$	$(6.97) \times 10^{-4}$
$2_5^+ \longrightarrow 0_1^+$	2242	1.8^{+7}_{-6}	1.2		

Ref. [6] we are led to confirm that it can be interpreted in the framework of the model. We note that the IBA-2 calculations closely reproduce the experimental value of the B(E2; $2_3^+ \longrightarrow 4_1^+$), which is not included in the decay scheme proposed in Refs. [8,9].

The scenario is different for the $\rho^2(2_4^+ \longrightarrow 2_1^+)$ and $\rho^2(2_5^+ \longrightarrow 2_1^+)$ strengths which are still known with limited precision. The comparison between the experimental and calculated B(E2) and B(M1) values for transitions de-exciting from the 2_4^+ and 2_5^+ states are also shown in Table IV. For both states, the electromagnetic transition probabilities are known with a large uncertainty so that the comparison with the calculation is not decisive. As a consequence, no definite conclusion could be drawn on the interpretation of the 2_4^+ as a member of the intruder band built on the 0_3^+ state, as suggested in Ref. [21]. We note also that no evidence of the $2_4^+ \rightarrow 0_3^+$ transition was reported so far and also in the present work no such transition was observed. Similarly, no definite conclusions can be drawn on the character of the 2_5^+ state. However because the 2_5^+ state does not de-excite to the 4_1^+ state, while the 2_4^+ state does, it seems preferable to associate the 2_4^+ as the 2^+ member of a $n_d = 3$ quintuplet and the 2_5^+ state to a coexisting configuration as suggested in Ref. [8]. The presence of a large E0 transition strength is considered as a signature of strong mixing between two states with different deformation (Ref. [27]) and according to Ref. [10] the ρ^2 values measured in ^{106}Pd are large enough to provide evidence for shape coexistence in this nucleus. We have therefore compared the experimental value of $\rho^2(0_i^+ \longrightarrow 0_f^+)$ with that evaluated in a simple mixing model, following the procedure described in Refs. [27,28]. The 0_2^+ and 0_1^+ states are assumed to be a linear combination of two basic configurations $|1\rangle$ and $|2\rangle$ of different deformations:

$$|0_1^+\rangle = b|1\rangle + a|2\rangle \quad |0_2^+\rangle = a|1\rangle - b|2\rangle \quad (a^2 + b^2 = 1). \tag{6}$$

It is possible to deduce an approximate expression for the monopole operator in terms of the deformation variables (β and γ) in a quadrupole deformation space [29]:

$$T(\hat{E}0) = \frac{3Z}{4\pi}\left(\beta^2 + \frac{5\sqrt{5}}{21\sqrt{\pi}}\beta^3 \cos 3\gamma\right). \tag{7}$$

In this approximation one obtains for $\rho^2(0_2^+ \longrightarrow 0_1^+)$ the expression:

$$\rho^2(0_2^+ \rightarrow 0_1^+) = \left(\frac{3Z}{4\pi}\right)^2 a^2(1-a^2)\Big[(\beta_1^2 - \beta_2^2) + \frac{5\sqrt{5}}{21\sqrt{\pi}}(\beta_1^3 \cos 3\gamma_1 - \beta_2^3 \cos 3\gamma_2)\Big]^2, \tag{8}$$

by neglecting the nondiagonal term $\langle 2|T(E0)|1\rangle$. The parameters β_1, γ_1 and β_2, γ_2 refer to the $|1\rangle$ and $|2\rangle$ unmixed states, respectively. As a first step, we have considered only the terms up to the second order in β. The values of the deformation parameters $\beta^2(0_1) = 0.050(2)$ and $\beta^2(0_2) = 0.069(3)$ have been extracted from Q^2 values obtained in a Coulomb excitation experiment [30]. Those can be expressed as a function of the β_1 and β_2 deformations of the unmixed state as follows:

$$\beta^2(0_1) = a^2\beta_1^2 + b^2\beta_2^2,$$
$$\beta^2(0_2) = b^2\beta_1^2 - a^2\beta_2^2. \tag{9}$$

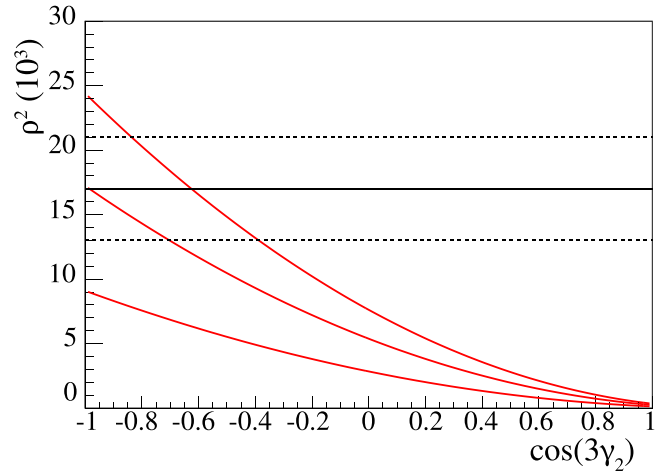

FIG. 9. Values of ρ^2 calculated as a function of the deformation parameter $\cos(3\gamma_2)$ for different values of the squared mixing amplitude a^2, assumed γ_1, β_1, and β_2 reported in Ref. [30]. The horizontal lines indicate the experimental value together with the $\pm\sigma$ statistical uncertainty.

Inserting the experimental values in Eqs. (8) and (9) the mixing coefficient a^2 was calculated to be $\approx$0.1. Because this value corresponds to a small mixing between the ground state and the 0_2^+ state, the assumption was made that the deformations of the mixed 0_1^+ (0_2^+) and unmixed $|1\rangle$ ($|2\rangle$) states are similar.

Under this hypothesis, and using the following assumptions, the value of $\rho^2(0_2^+ \longrightarrow 0_1^+)$ can be calculated using Eq. (8). The value of deformation parameter of the ground state $\gamma = 20(2)^\circ$ was taken from Ref. [30]. We assume in the calculations the values for $\sqrt{\beta^2(0_1)} = 0.22$, $\gamma_1 = 20^\circ$, and $\sqrt{\beta^2(0_2)} = 0.26$ while the deformation parameter γ_2 was varied in a reasonable range for three different sets of values for a^2, corresponding to small mixing. The calculated values of $\rho^2(0_2^+ \longrightarrow 0_1^+)$ are compared to the experimental one in Fig. 9. The comparison with the experimental value implies $\gamma_2 \approx 50^\circ$ for the $|2\rangle$ state, and hence for the 0_2^+ state. This result would imply the coexistence of different shapes, triaxial for the ground state and oblate for the first excited 0^+ state, in agreement with the conclusions drawn in Ref. [10].

V. CONCLUSIONS

In summary, the E0 transitions in ^{106}Pd between both 0^+ and 2^+ states have been investigated in a decay spectroscopy experiment at the INFN Legnaro National Laboratories. The experiment used the newly installed SLICES setup and an HPGe detector for the measurement of conversion electrons and γ rays, respectively. A set of K-conversion coefficients and monopole transition strengths was extracted. The obtained data allow us to discriminate between the two discrepant α_K values reported in the literature for the $2_3^+ \longrightarrow 2_1^+$

transition. The first observation of the E0 transitions from the fourth 0^+ state is reported but only limits on ρ^2 values were extracted because of the limit on its lifetime. In ^{104}Pd isotope hints of the existence of the fourth 0^+ state at 2101 keV were found reanalyzing the data of an experiment previously performed.

Calculations of the ρ^2 values in ^{104,106}Pd were performed in the framework of the interacting boson model, using the parameters reported in Ref. [6] and the monopole boson charges extracted in the present work. The agreement between theoretical results and measurements is good, once the experimental 0_3^+ state is considered as an intruder state. For both ^{104,106}Pd isotopes predicted states having a structure resembling that of states belonging to the $n_d = 2, 3$ multiplets of the U(5) limit have been associated with the experimental states. Further experimental studies to get more information about the excited 0^+ and 2^+ states in the neighboring palladium isotopes are needed for better understanding of the underlying structure of these states.

The experimental value of $\rho^2(0_2^+ \longrightarrow 0_1^+)$ was also compared to that calculated in a simple two-state mixing model. The conclusion is that the mixing between the first two 0^+ states in this nucleus is small. The coexistence of different shapes is also implied.

ACKNOWLEDGMENTS

The authors would like to thank the staff of the CN accelerator (LNL) for providing the beams used in this experiment, M. Loriggiola for producing the targets, and the mechanical workshops of the INFN divisions of Florence and the University of Camerino for their contribution. E.R.G. wishes to acknowledge the Centro E. Fermi for financially supporting his postdoctoral fellowship through the project BESTRUCTURE. This work was supported partly by the Basic Science Research Program through the National Research Foundation of Korea (NRF) funded by the Ministry of Education, Grant No. 2020R1A6A3A03039081.

[1] D. Sohler, I. Kuti, J. Timar, P. Joshi, J. Molnar, E. S. Paul, K. Starosta, R. Wadsworth, A. Algora, P. Bednarczyk, D. Curien, Z. Dombradi, G. Duchene, D. B. Fossan, J. Gal, A. Gizon, J. Gizon, D. G. Jenkins, K. Juhasz, G. Kalinka *et al.*, Phys. Rev. C **85**, 044303 (2012).
[2] C. Y. He, B. B. Yu, L. H. Zhu, X. G. Wu, Y. Zheng, B. Zhang, S. H. Yao, L. L. Wang, G. S. LI, X. Hao, Y. Shi, C. Xu, F. R. Xu, J. G. Wang, L. Gu, and M. Zhang, Phys. Rev. C **86**, 047302 (2012).
[3] Y. X. Luo *et al.*, Nucl. Phys. A **919**, 67 (2013).
[4] P. Banerjee, S. Ganguly, M. K. Pradhan, M. MoinShaikh, H. P. Sharma, S. Chakraborty, R. Palit, R. G. Pillay, V. Nanal, S. Saha, J. Sethi, and D. C. Biswas, Phys. Rev. C **92**, 024318 (2015).
[5] K. Kim, A. Gelberg, T. Mizusaki, T. Otsuka, and P. von Brentano, Nucl. Phys A **604**, 163 (1996).
[6] A. Giannatiempo, A. Nannini, and P. Sona, Phys. Rev. C **58**, 3316 (1998).
[7] F. Iachello and A. Arima, *The Interacting Boson Model* (Cambridge University Press, Cambridge, UK, 1987).
[8] P. E. Garrett, J. L. Wood, and S. W. Yates, Phys. Scr. **93**, 063001 (2018).
[9] F. M. Prados-Estevez, E. E. Peters, A. Chakraborty, M. G. Mynk, D. Bandyopadhyay, N. Boukharouba, S. N. Choudry, B. P. Crider, P. E. Garrett, S. F. Hicks, A. Kumar, S. R. Lesher, C. J. McKay, M. T. McEllistrem, S. Mukhopadhyay, J. N. Orce, M. Scheck, J. R. Vanhoy, J. L. Wood, and S. W. Yates, Phys. Rev. C **95**, 034328 (2017).
[10] E. E. Peters, F. M. Prados-Estévez, A. Chakraborty, M. G. Mynk, D. Bandyopadhyay, S. N. Choudry, B. P. Crider, P. E. Garrett, S. F. Hicks, A. Kumar, S. R. Lesher, C. J. McKay, J. N. Orce, M. Scheck, J. R. Vanhoy, J. L. Wood, and S. W. Yates, Eur. Phys. J. A **96**, 52 (2016).
[11] G. Colvin, F. Hoyler, and S. Robinson, J. Phys. G.: Nucl. Phys. **13**, 191 (1987).
[12] N. Marchini, A. Nannini, M. Ottanelli, A. Saltarelli, M. Rocchini, G. Benzoni, E. R. Gamba, A. Goasduff, A. Gottardo, T. Krings, and M. Perri, Nucl. Instrum. Methods Phys. Res., Sect. A **1020**, 165860 (2021).
[13] [https://www.lnl.infn.it/en/cn-2/].
[14] T. Kibèdi, T. W. Burrows, M. B. Trzhaskovskaya, P. M. Davidson, and C. W. Nestor, Nucl. Instrum. Methods Phys. Res., Sect. A **589**, 202 (2008).
[15] K. Farzin, H. Handenberg, H. Möllmann, K. Uebelgünn, and H. V. Buttlar, Z. Phys. A At. Nucl. **326**, 401 (1987).
[16] J. Smallcombe *et al.*, Eur. Phys. J. A **54**, 165 (2018).
[17] D. D. Frenne and A. Negret, Nucl. Data Sheets **109**, 943 (2008).
[18] J. Blachot, Nucl. Data Sheets **108**, 2035 (2007).
[19] M. E. Bellizzi, A. Giannatiempo, A. Nannini, A. Perego, and P. Sona, Phys. Rev. C **63**, 064313 (2001).
[20] G. Lhersonneau, J. C. Wang, S. Hankonen, P. Dendooven, P. Jones, R. Julin, and J. Aysto, Phys. Rev. C **60**, 014315 (1999).
[21] Y. Wang, P. Dendooven, J. Huikari, A. Jokinen, V. S. Kolhinen, G. Lhersonneau, A. Nieminen, S. Nummela, H. Penttila, K. Perajarvi, S. Rinta-Antila, J. Szerypo, J. C. Wang, and J. Aysto, Phys. Rev. C **63**, 024309 (2001).
[22] P. E. Garrett, J. Phys. G: Nucl. Part. Phys. **43**, 084002 (2016).
[23] A. Giannatiempo, A. Nannini, P. Sona, and D. Cutoiu, Phys. Rev. C **52**, 2969 (1995).
[24] A. Giannatiempo, Phys. Rev. C **98**, 034305 (2018).
[25] T. Otsuka and N. Yoshida, The Program NPBOS, Japan Atomic Energy Research Institute, Report No. JAERI-M85-094 (1985).
[26] T. Kibèdi and R. Spear, Atomic Data and Nucl. Table **89**, 77 (2005).
[27] J. L. Wood, E. F. Zganjar, C. D. Coster, and K. Heyde, Nucl. Phys. A **651**, 323 (1999).
[28] A. Giannatiempo, A. Nannini, A. Perego, P. Sona, H. Mach, B. Fogelberg, M. J. G. Borge, O. Tengblad, L. M. Fraile, A. J. Aas, and K. Gulda, Phys. Rev. C **72**, 044308 (2005).
[29] A. S. Davydov, V. S. Rostovsky, and A. A. Chaban, Nucl. Phys. **27**, 134 (1961).
[30] L. Svensson, C. Fahlander, L. Hasselgren, A. Bäicklin, L. Westerberg, D. Cline, T. Czosnyka, C. Wu, R. Diamond, and H. Kluge, Nucl. Phys. A **584**, 547 (1995).